Cornell University

Mechanical Design for CCAT-p Wall Climbing Robot

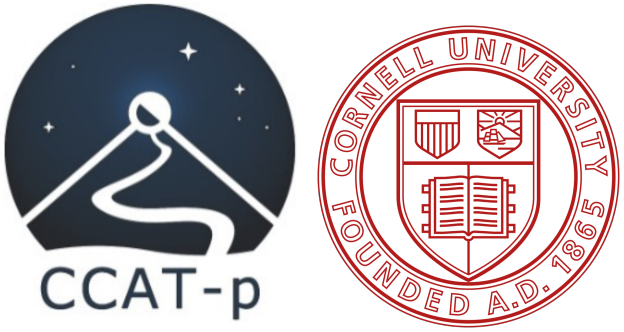

Prepared By:

Zijie Chen

Hyunji Kim

Alex Zhou

Supervisor: Prof. Dmitry Savransky

Sibley School of Mechanical and Aerospace Engineering

May 20, 2019

Abstract

CCAT-p is a 6-meter diameter telescope that will be operational in 2021 and built on a site on Cerro Chajnantor in the Atacama Desert of northern Chile. The telescope consists of 2 aluminum panel mirrors which are composed of 78 and 87 separate panels. As it is crucial that all of the panels are aligned correctly for the proper function of the telescope, we are designing a robot that would assist in the metrology of these mirror panels. The team is divided into two subteams - the mechanical team and the controls team. This document will report the work of the mechanical team completed between September 2018 and May 2019. Zijie Chen was in charge of the FEA portions, Hyunji Kim was the mechanical team lead and aided in different tasks, and Alex was in charge of the CAD of the robot chassis and dynamic simulations of the tethers.

Contents

List of Figures **iii**

List of Tables **iv**

1 Introduction **1**
1.1 Background 1

2 Methodology **3**
2.1 Design and Decision Criteria 3
2.1.1 Requirements 3
2.2 Materials and Apparatus 4
2.2.1 Puck 4
2.2.2 Eddy current sensor 5
2.2.3 Building materials 5
2.2.4 Testing plan 5
2.3 Procedure 8
2.3.1 Robot Design 8
2.3.2 Safety Tether System 13
2.3.3 Error Budget 16
2.3.4 Simulations 17

3 Results **24**
3.1 Conclusion 24
3.1.1 Robot construction 24
3.1.2 Simulation test 25
3.1.3 Future Plan 25

Bibliography **26**

List of Figures

1.1 Prototype 1 2

2.1 Friction Test: Coefficient of Friction vs. Number of Rubber Layers 6
2.2 Fan Thrust Test Setup Diagram 7
2.3 Fan motor specifications 8
2.4 M1 Mirror Panel Dimensions (units in mm) 9
2.5 M2 Mirror Panel Dimensions (units in mm) 10
2.6 Free body diagram of the robot to determine the thrust requirement 11
2.7 Equations for the minimum thrust requirement of the fans 12
2.8 Cross-sectional view of the puck tower 12
2.9 Top view of the puck tower 13
2.10 Exploded view of the puck tower 14
2.11 Side view of the tether placement 15
2.12 Front view of the tether placement 15
2.13 Thermal FEA of puck 19
2.14 Top view of puck tower model and fixed part shown in blue 20
2.15 Overall static result on deformation of all parts. The gradient bar is shown on left top corner (units in meter) 21
2.16 Force condition: tensile pressure applied on the red area of puck tower 22
2.17 Failure test result: the maximum stress on puck tower (units in Pa) 22
2.18 Simulator result for tether system 23

3.1 Exploded view of the robot 24

List of Tables

2.1 Dragon Skin Friction Test 6
2.2 Materials properties of puck tower 20
2.3 The detailed results of deformation between center of puck and bottom of probe 21

Chapter 1

Introduction

The CCAT-p wall climbing robot is a sub-project of a new observatory which is currently under construction in Chile. The telescope of the observatory has two mirrors, which are composed of 78 and 87 separate aluminum panels. Each mirror panel has four actuators behind its reflective surface that adjust the orientation and cancel the thermo-deformation of the panels. As a prerequisite of the mirror re-calibration procedure, the absolute orientation and location of each mirror needs to be measured. This is achieved by a laser based autonomous measuring system provided by Etalon, the company that is contracted to build the CCAT-p telescope. The characteristic of the aluminum panels make direct measurement of the surface via laser impossible, so a specialized reflector must be used to make measurements of the mirror. Due to the orientation variability of the mirror panels, environmental conditions, measurement constraints, and the size of the panels, it has been determined that an autonomous climbing robot that can carry the reflector to specific points on the mirror is the best method for achieving this metrology. The main task of our CCAT-p wall climbing robot is to carry the retro-reflector (i.e. puck) and place it on multiple desired positions on each mirror surface.

1.1 Background

CCAT-p is a 6-meter diameter telescope that will be operational in 2021 and built on a site on Cerro Chajnantor in the Atacama Desert of northern Chile. The telescope is being constructed under the partnership of Cornell University, Vertex Antennentechnik GmbH of Germany, and additional institutes in the U.S., Canada, Germany, and Chile. At the inception of this climbing robot project, several different climbing methods were explored, including electromagnetic robot, sticky feet robot, and suction robot. However, it was determined that a fan suction powered climbing method was the most appropriate for our requirements. Between spring of 2018 and fall of 2018, the first prototype of the climbing robot was built, as seen in Figure 1.1.

In this prototype, the robot was powered by 1 fan, and the puck was housed externally on an actuated arm. Between Fall of 2018 and Spring of 2019, our team has been working on the second prototype of this robot, with several improvements from the first prototype.

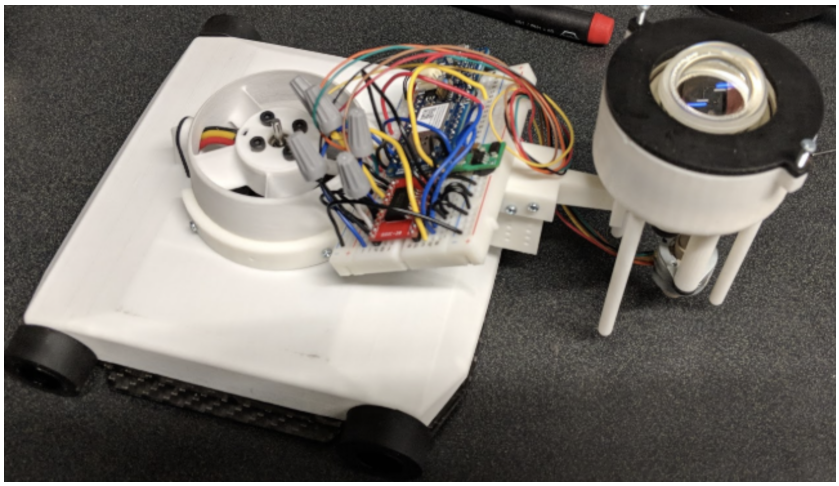

Figure 1.1: *Prototype 1*

Chapter 2

Methodology

2.1 Design and Decision Criteria

The climbing robot's design is determined by environmental requirements and measurement requirements, and are tested using different methods.

2.1.1 Requirements

The CCAT-p Climbing operates under many requirements, which are listed below.

1. CCAT-p environmental conditions
    - Operating air temperature: -21° C to +9° C
    - Survival air temperature: -30° C to +25° C
    - Air pressure: 50 to 53 kPa
    - Relative humidity: 0 to 90%
    - The observatory provides single phase 230 V, 50 HZ AC power. Observatory plug receptacles are CEE 7/3.
2. Measurement Program
    - Retro-reflector must be placed at a minimum of 9 points per panel (over Z adjusters.
    - Primary mirror: 87 panels, approximately 30° incline
    - Secondary mirror: 78 panels, approximately 20° overhang
    - Each panel face is approximately 675 x 675 mm. Placement repeatability is 1 cm absolute Retro-reflector z-axis offset from mirror surface measurement or repeatability is 0.5 micrometers RMS.
    - If z-axis offset is being established via measurement, z-offset measurements must be synchronized with Etalon measurements to within 1 ms, not accounting network latency.
    - Total mirror measurement time should not exceed 1 hour per mirror.

- The robot must navigate in a pre-planned path across each mirror surface, stopping for each measurement.
- At each measurement position the robot control system must broadcast a start single measurement request to the Etalon multline server.
- The Retro-reflector must be unobscured to the laser measurement system (60 degree of clearance around).
- The robot cannot inject greater than 1 micrometer RMS of unfilterable vibration into the mirror surface during measurements.
- The robot must measure multiple elevation angles in one night without human interaction.

3. Safety and Operability

- The robot cannot become detached from the mirror surface, or if detachment occurs cannot impact any mirror or observatory surface or equipment
- The robot must be capable of completing a full measurement cycle of one mirror without interruption (i.e., the robot must be continuously operable for the duration of one mirror measurement cycle)
- The robot cannot drive off of the edge of the mirror
- In the event of any operational anomaly, the robot must be capable of placing itself in a safe mode
- Safe mode is defined as the robot meeting all safety requirements in a full power-off state
- An operational anomaly is defined as a violation or potential imminent (within 1 s) violation of any safety or operability requirement
- The robot must be capable of traversing the mirror surfaces, including any surface gaps or defects
- The robot cannot be capable of scratching, scuffing or in any other way damaging or affecting the performance of any mirror surface
- The robot must be capable of carrying out the measurement program (Sec. 2) in the full range of environmental conditions (Sec. 1)
- The robot must survive and be capable of placing itself into a safe mode in the event of total loss of observatory power
- The robot must reply to Observatory Control System alarms/alerts (interface must be provided by project)
- The robot must operate safely in the event of an earthquake, up to accelerations of 1 g.

2.2 Materials and Apparatus

2.2.1 Puck

The puck is the retro-reflector provided by the Etalon laser measuring system and is the main payload of the robot. It is a spherical glass with an outer diameter of 30 mm. The puck

requires at least 60 degrees of clearance around the z-axis and no structures are to cross the clearance of the puck during the measurement sequence.

2.2.2 Eddy current sensor

In order to fulfill the precision requirements of the z-axis offset measurements, our team has decided to use a distance sensor called the eddy current sensor. This is a magnetic based sensor which measures the distance between the measured surface (the mirror panel) and the probe's bottom surface. The range of the sensor is 0.3 mm to 2mm and the resolution is 0.02% at most. By using the eddy current sensor, we can control the uncertainty of the measured distance between the puck and the mirror surface. The remaining uncertainty can only come from the distance between the punk and the sensor, which can be designed through the robot's structure to minimize the uncertainty of the distance between the eddy current sensor and the puck.

2.2.3 Building materials

Tires materials

The wheel tires are the only parts of the robot that will make contact with the mirror surface. According to the safety requirements, the tire materials must not contaminate the mirror surface. However, the material should have a high enough coefficient of friction so that the robot can reliably attach to the mirror. Hyunji have chosen a material called Dragon-Skin 10NV, which is a silicone rubber material produced by Smooth-On. Dragon-Skin can be molded into any shape and the method of manufacturing the molds of the wheels is 3D printing. The material has a 6-month shelf life and it was opened on Jan. 28th 2019.

Puck tower & ZERODUR

From part 2.2.2 we know that the only source of the z-axis offset uncertainty is the distance between the probe of the eddy current sensor and the Puck. Although we cannot assure where the measurement happens between these two parts, we can assume that the critical distance is from the geometric center of the puck to the bottom surface of the probe.

The three sources of uncertainty are thermal-deformation, tilting and vibration. In order to minimize the thermal effect we want the coefficient of thermal-expansion of the structural material to be as small as possible. Thus the mechanical team have choosen a low expansion glass material called ZERODUR, which is produced by Schott. This special glass material has a very low CTE and is often used in aerospace application where high temperature fluctuations are expected in mission critical areas. We will be using the material as the core structure of the puck tower. According to the quote from the manufacturer, the ZERODUR part has 14 weeks of lead time.

2.2.4 Testing plan

Wheel Friction Test

The goal of the Dragon-Skin friction test experiment was to find the coefficient of friction between Dragon-Skin silicone rubber and the aluminum panel. Through testing, we observed

that the rubber layers would rub off on the panel mirror, changing the coefficient of friction depending on the number of passes the rubber has gone over the mirror surface. The test first started with the molding of Dragon-Skin with a weight in the center. After the material was prepared, a tilt friction test was performed by placing the material on the aluminum mirror panel and then tilting the panel until the material slid. The angle of tilt was measured in order to calculate the coefficient of friction. The results are in Table 2.1 and graph 2.1:

Table 2.1: *Dragon Skin Friction Test*

Mirror Surface	**Number of Rubber Layers**	**Average Coefficient of Friction**	**Uncertainty in Coefficient of Friction**
Clean	0	0.92	0.03
3 Rubber Layers	3	0.86	0.03
6 Rubber Layers	6	0.84	0.03
9 Rubber Layers	9	0.80	0.03
12 Rubber Layers	12	0.80	0.03
15 Rubber Layers	15	0.80	0.03

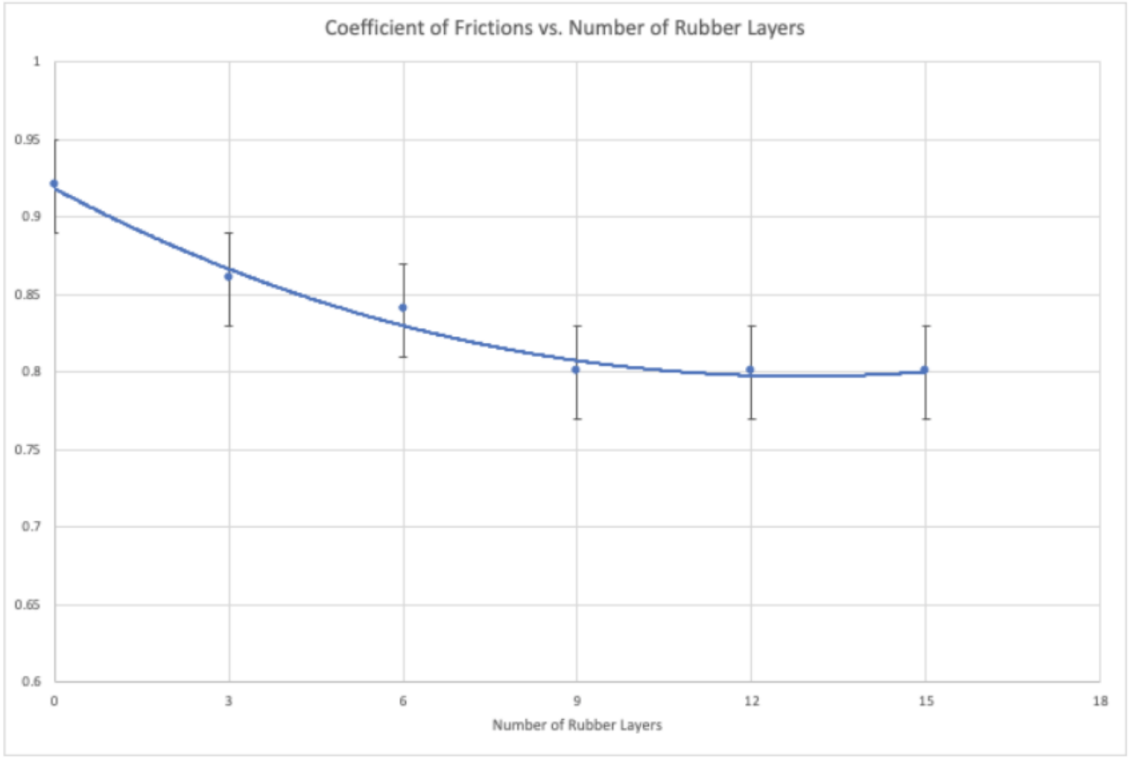

Figure 2.1: *Friction Test: Coefficient of Friction vs. Number of Rubber Layers*

However, the rubber's residue on the mirror surface is a violation of a requirement, so a different method of Dragon-Skin's curing was explored. After testing, it was determined that treating the curing surface of the mold with liquid acrylic and letting it dry completely

allows Dragon-Skin to fully cure and not contaminate the mirror's surface of layers of rubber. Therefore, the final result of the wheel friction test was a coefficient of friction of 0.92 between Dragon-Skin and the aluminum panels.

Robot Speed Test

A speed test was done by Sparsh in order to confirm that the speed performance and acceleration performance of the robot meets the requirements. The test was done by first weighing the robot to be 1kg and then driving the robot in a straight line for a certain distance and then measuring the elapsed time. The result showed that the robot's speed exceeds 100cm/s, which fully meets the measurement requirements.

Fan Thrust Test

The goal of the fan thrust test was to determine which kind of impellers would produce sufficient thrust. The first test was done under standard air pressure (101kPa). Future tests in vacuum chamber are planned to simulate the actual working conditions (50kPa). The basic principle of the fan experiment is shown in Figure 2.2:

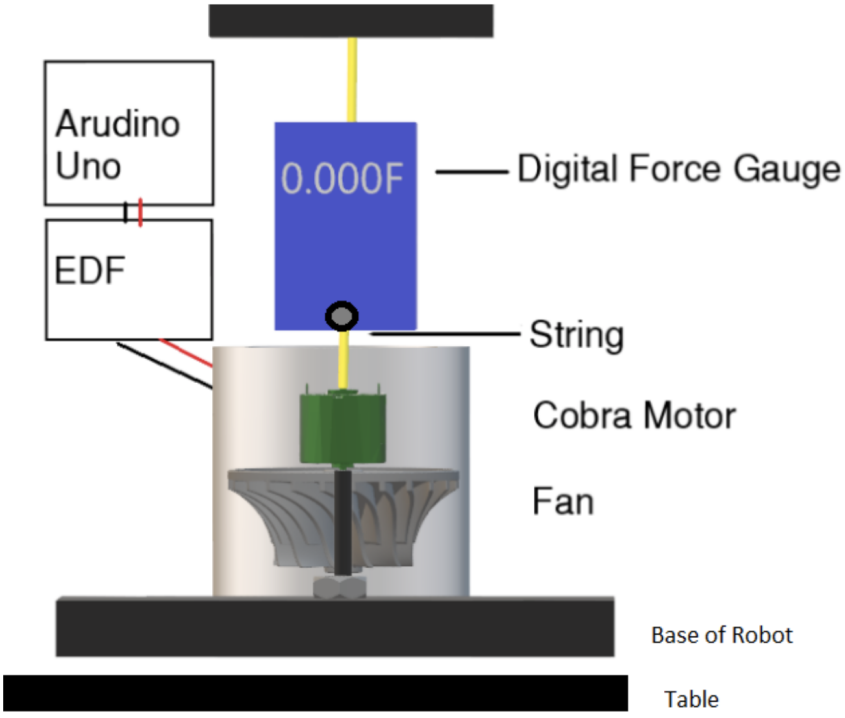

Figure 2.2: *Fan Thrust Test Setup Diagram*

During the experiment, different fans were installed on a testing unit which was composed of the motor, the electronics, and other structures including a bottom plate which simulated the robot chassis. The bottom plate was kept 3mm above a flat surface and this distance was fixed by gaskets. When the fan was running, the testing unit was lifted by the handle of the force gauge. The value on the force gauge at the time of detachment from the surface

indicated the maximum thrust generated by the fans. The thrust force was then calculated by subtracting the weight of the test unit from the force gauge reading. By comparing the thrust force of different fan designs, we quantified their performance. The test heavily relies on the state of the motor, so in every test, the rotational speed of the motor was the same. The specifications of the motor used during the experiment are in Figure 2.3.

Cobra 2208/26 Motor Specifications	
Stator Diameter	22.0 mm (0.866 in)
Stator Thickness	8.0 mm (0.315 in)
Number of Stator Slots	12
Number of Magnet Poles	14
Motor Wind	26 Turn Delta
Motor Kv Value	1550 RPM per Volt
No Load Current (Io)	0.53 Amps @ 8 Volts
Motor Resistance (Rm) per Phase	0.150 Ohms
Motor Resistance (Rm) Phase to Phase	0.100 Ohms
Maximum Continuous Current	15 Amps
Max Continuous Power (2-cell Li-Po)	115 Watts
Max Continuous Power (3-cell Li-Po)	165 Watts
Motor Weight	46.5 grams (1.64 oz.)
Outside Diameter	27.7 mm (1.091 in.)
Shaft Diameter	3.17 mm (0.125 in.)
Motor Body Length	24.0 mm (0.945 in.)
Overall Shaft Length	38.0 mm (1.496 in.)
Motor Timing	5-10 degrees
PWM Frequency	8 KHz

Figure 2.3: *Fan motor specifications*

2.3 Procedure

2.3.1 Robot Design

Wheelbase

The robot is not allowed to drive off the mirror surface so the dimensions of the robot chassis are be limited by the size of mirror panels. Based on the dimensions of the mirror panels, the mechanical team have decided that the maximum track of the robot is 160mm and maximum wheelbase is 190mm. Figure 2.4 and Figure 2.5 shows the dimensions of these panels including the measurement points.

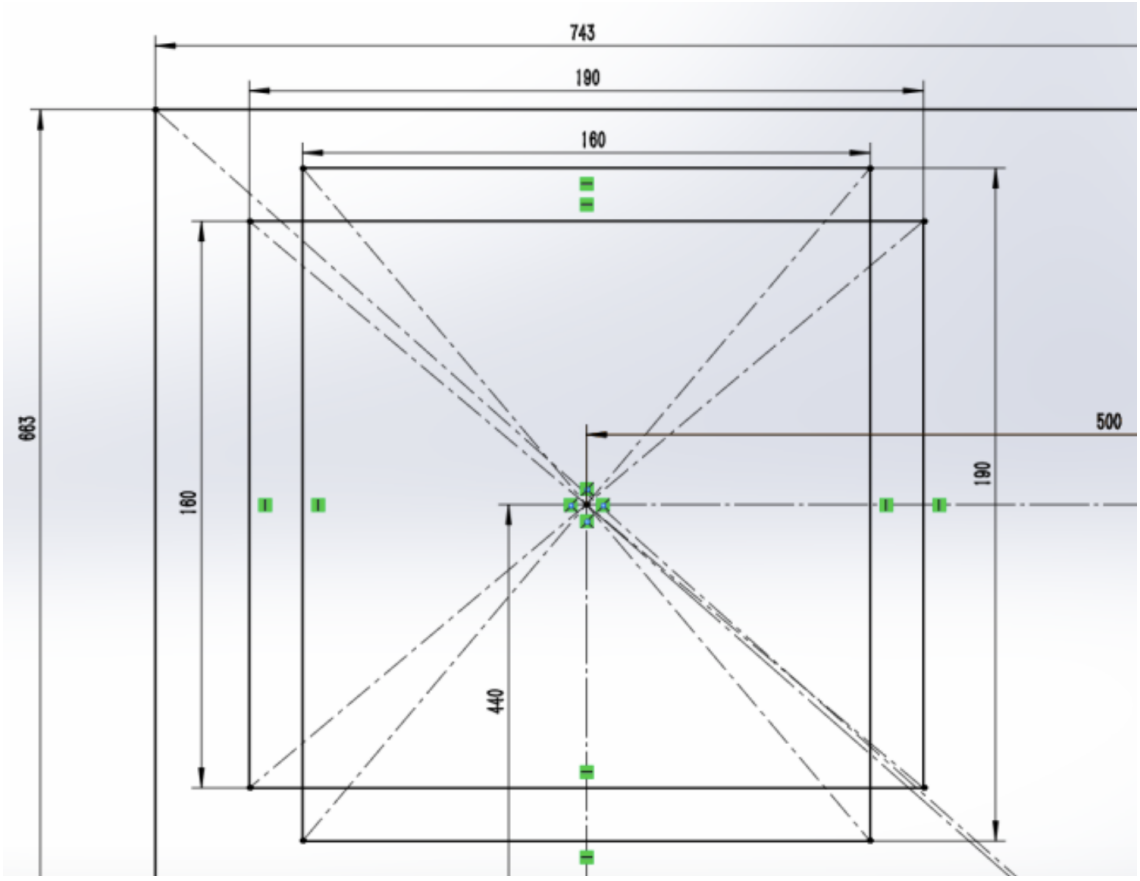

Figure 2.4: *M1 Mirror Panel Dimensions (units in mm)*

Chassis Height

The gap height between the chassis and mirror may affect the performance of the fans. According to the testing results from the summer of 2018, the chassis height was determined to be optimal at 3mm.

Motion System

The robot is driven by four brush motors which can be controlled independently. The robot is steered using differential steering. The motors we have chosen are the Pololu Micro Metal Gearmotors, and have built-in gearboxes and the gear ratio will be dependent on the speed and torque requirements of the final robot design. From a rough estimation of the total distance the robot needs to travel, the speed requirement of the robot is determined to be 150 mm/s. The corresponding gear ratio is 1:75. The robot was designed to be operated with external power supply, because the battery with enough capacity will make the robot weight unacceptable.

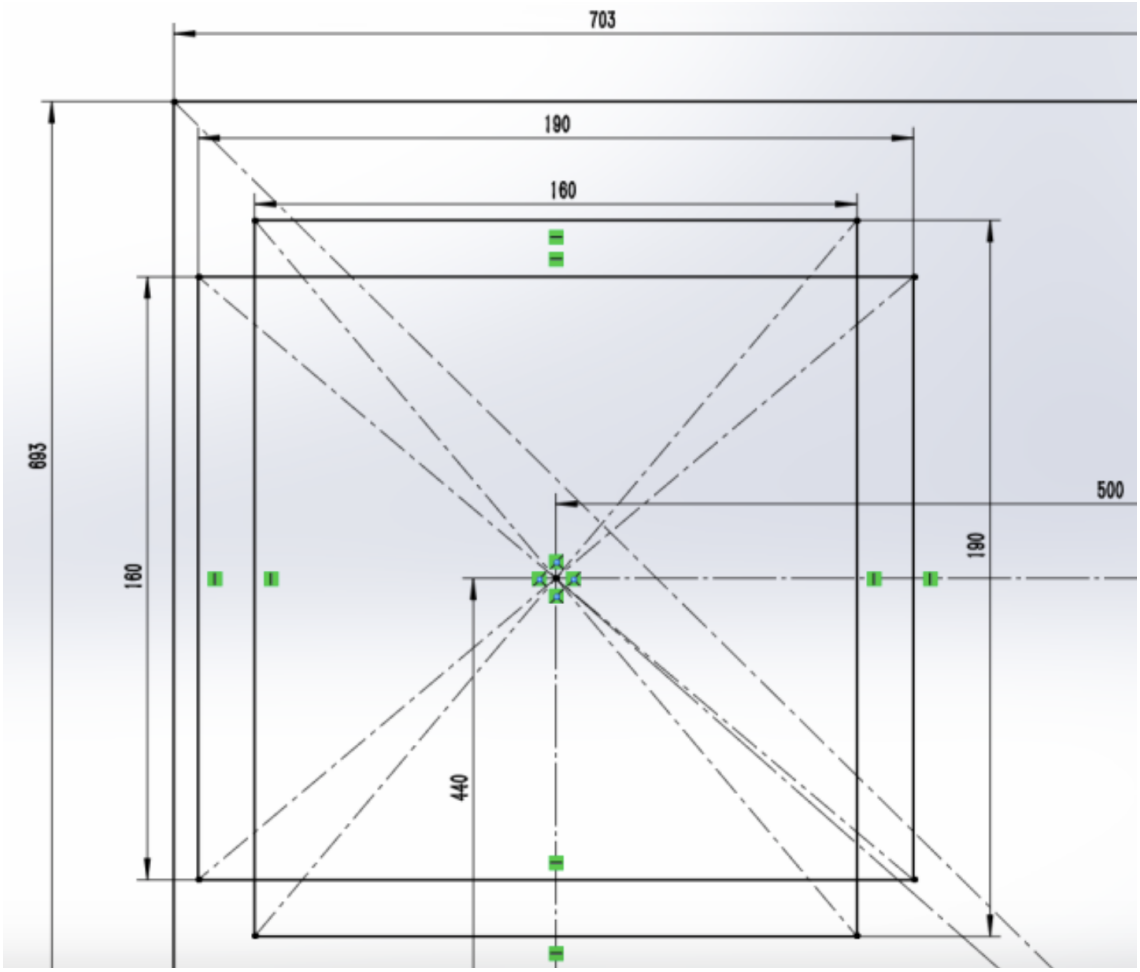

Figure 2.5: *M2 Mirror Panel Dimensions (units in mm)*

Edge Sensors

According to the sensor design from the controls team, the robot will have an edge sensing mechanics as a part of the safety system to prevent the robot from driving off the mirrors. There will be 4 edge-sensing units placed at the corners of the robot. Each unit has a light sensor and an led light. During operation, the LED will illuminate a small area below the sensor so it can sense the difference in reflectivity between mirror panels and gaps. The mounts for these edge sensors are to be 3D printed and attached to the main chassis of the robot with M2 screws.

Fans

The fans are the core components for the wall climbing robot. Working as impellers, the fans will suck in air from the gap between chassis and mirrors and expel it from the top of the robot. This creates a low pressure zone below the chassis and a thrust which will create a normal force that pushes the robot into the mirror surface. Using the following FBD shown

in Figure 2.6, we can determine the minimum thrust needs to be created by each fan.

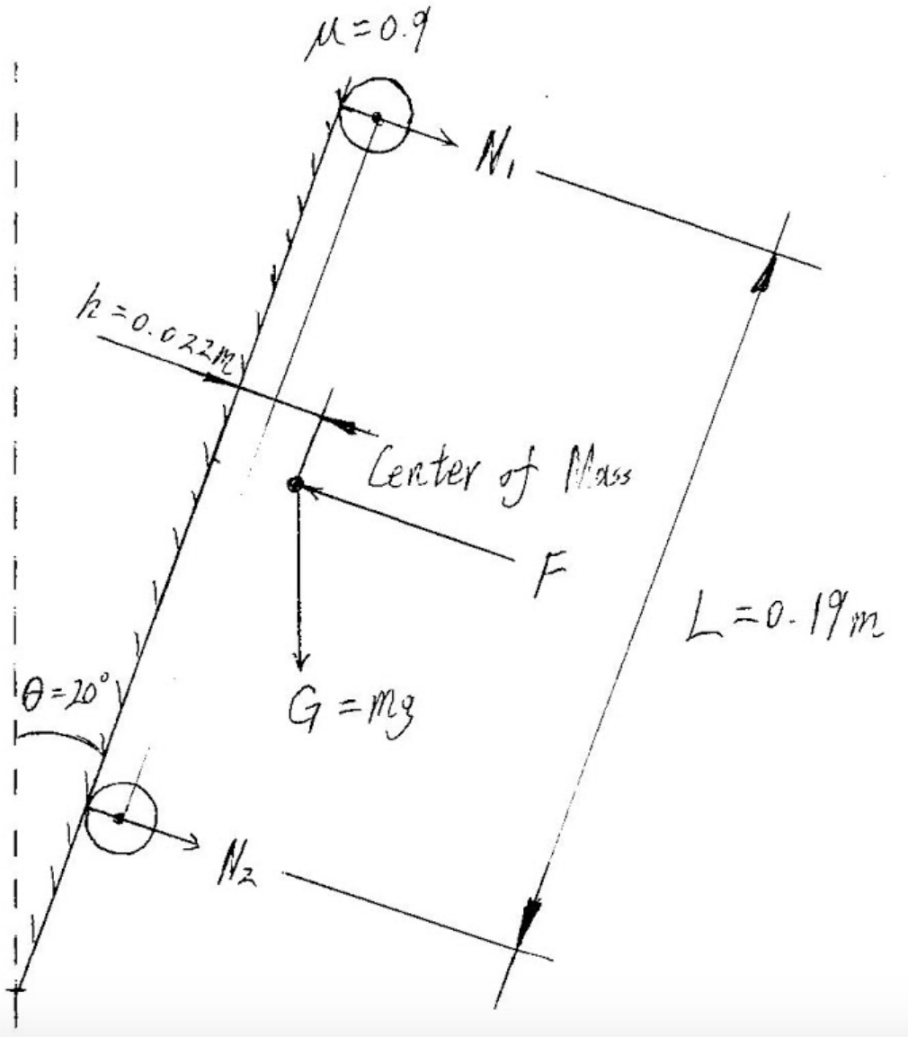

Figure 2.6: *Free body diagram of the robot to determine the thrust requirement*

The robot is not allowed to fall or slide on the mirror, so the minimum thrust must satisfy the following equations shown in Figure 2.7:

Where $N1$ and $N2$ are the normal load on the front and rear tires. L is the wheelbase of the robot and $L = 0.19m$. m is the total mass of the robot and we will use $m = 1kg$. $g = 9.81m/s^2$. θ is the overhang angle. h is the height of the robot CoM, and $h = 0.022m$. Solve for the thrust F and we will have $F = 26N$, which means the minimum thrust needs to be created by each fan is $13N$.

Puck Tower

The placement of the retro reflector and the eddy current sensor is critical to the performance of the robot. Because the retro reflector is a spherical object with no connectors, we cannot

$$\begin{cases} N_1 \cdot L + mg\left(\frac{L}{2}\sin\theta + h\cos\theta\right) = \frac{L}{2}\cdot F \\ N_2 \cdot L + mg\left(\frac{L}{2}\sin\theta + h\cos\theta\right) = \frac{L}{2}\cdot F \end{cases}$$

$$(N_1 + N_2)\cdot \mu = mg\cos\theta$$

$$\frac{L}{\mu}\cos\theta + \frac{L}{2}\sin\theta + h\cos\theta = \frac{L}{2}\cdot\frac{F}{mg}$$

Figure 2.7: *Equations for the minimum thrust requirement of the fans*

use screws to mount it on our robot. Thus a customized structure (i.e. puck tower) is required to contain the puck. The puck tower design was based on the following rules:

The geometric center of the puck and the eddy current sensor should coincide;

The distance from the puck to the eddy current sensor should be minimized;

The puck can not slide in the holder, which means minimum clamping force needs to be satisfied in any orientation.

The sectional view of the current puck tower design is shown Figure 2.8, and a top view is shown in Figure 2.9.

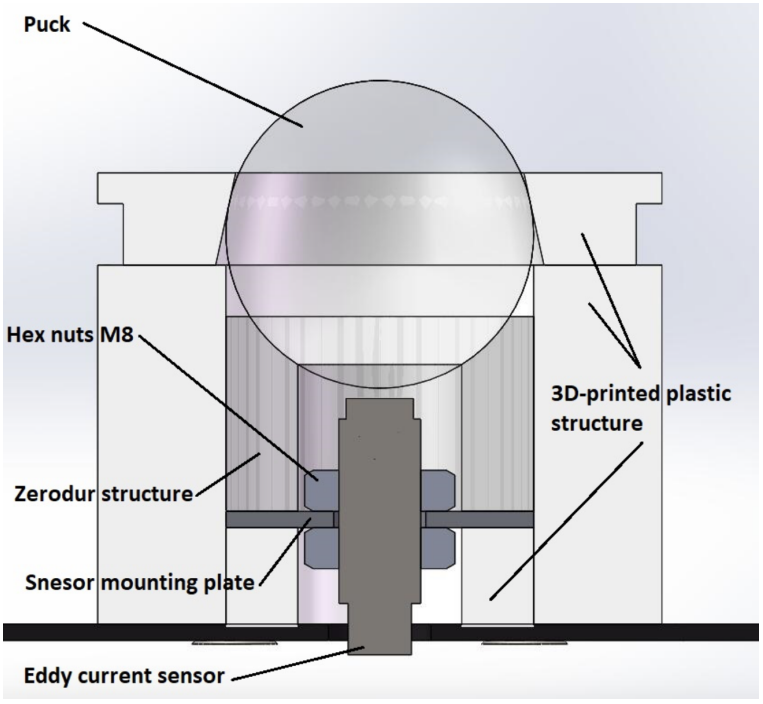

Figure 2.8: *Cross-sectional view of the puck tower*

The main structure of the puck tower can be divided into 2 concentric parts: The inner ring is the support of the puck and eddy current sensor. It has three layers and the upper one

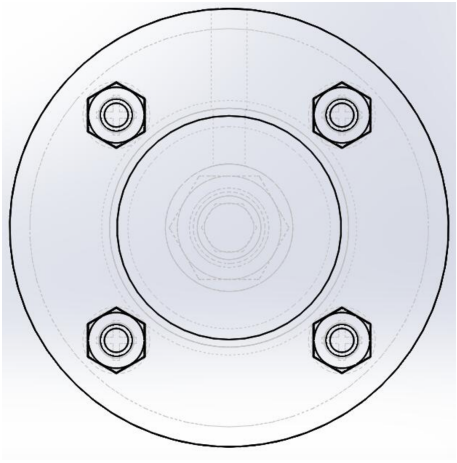

Figure 2.9: *Top view of the puck tower*

is the ZERODUR part. The outer ring is made by two separate parts and together they will mount the puck tower on the robot. The puck tower is fastened by screws and the assembly process are shown in Figure 2.10:

Other Payloads

Eddy Current Sensor Conditioner

The probe of the eddy current sensor needs a conditioner to work properly. The eddy current sensor conditioner is a high volume payload which significantly affects the robot's design. The conditioner must be on the body of the robot and cannot be offloaded because of the restriction on the length of wire connection between the probe and the conditioner. Based on the specifications of the eddy current sensor, it may need a heating system to meet the working temperature requirements of the eddy current sensor conditioner.

Electronics

The Raspberry Pi 3B serve as the onboard computer of the robot. It needs 5V DC power so a transformer is required. The wheel motors will also needs micro controllers to adjust speed and they may have encoders (depends on the control plan of the robot). All electronics except the Raspberry Pi will be installed on a single breadboard. The current CAD model of the robot does not include it, however, because the final dimensions of the breadboard is not decided by now.

2.3.2 Safety Tether System

The tether systems is the main safety measure of the robot and there will two separate tether systems for each mirror. Two tethers are connected to the robot during the entire measurement and the mounting points are near the diagonal points of the mirror. Each of the mounting points will have a motorized reel and other electronics. The tethers are steel cables and they are allowed to be disassembled from the robot. If robot detach from the mirror (this can be detected by the IMU), it will send a signal to the tether system and activate the motor. The reel will then quickly retract the tethers in both directions and the

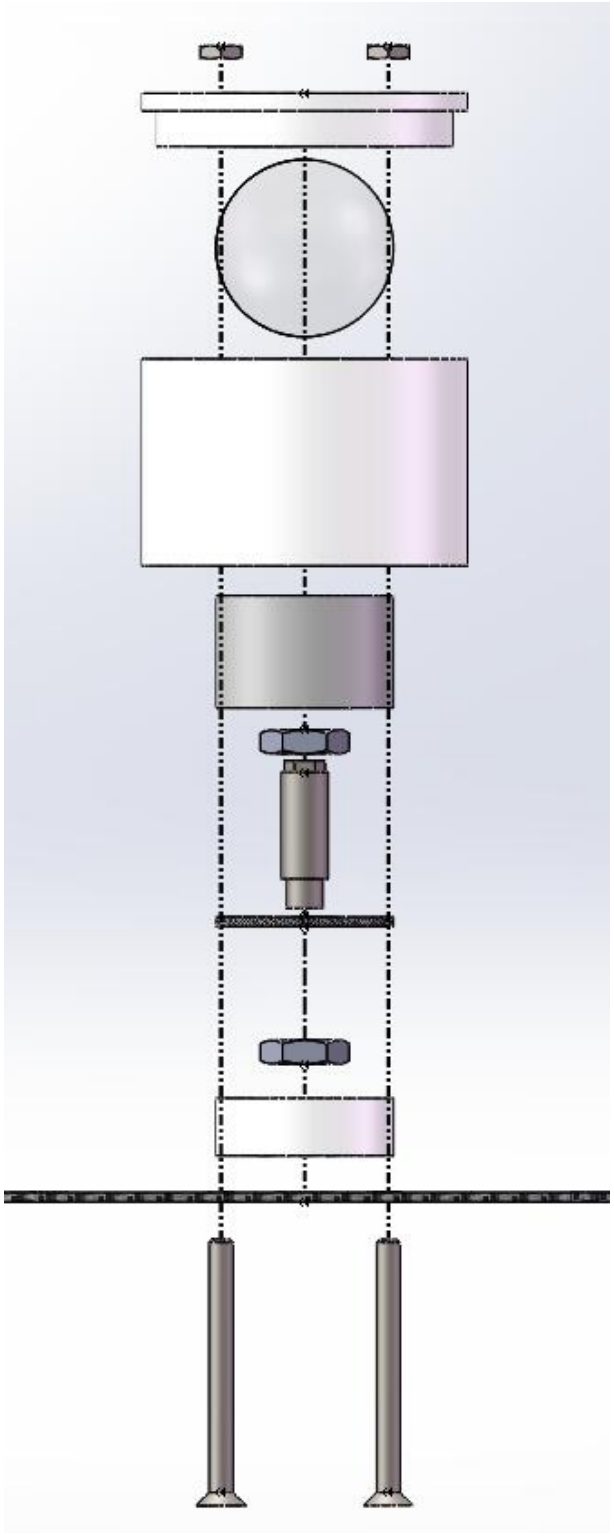

Figure 2.10: *Exploded view of the puck tower*

robot will be hung in the air.

The locations of the tether mounting points are shown in Figure 2.11 and Figure 2.12.

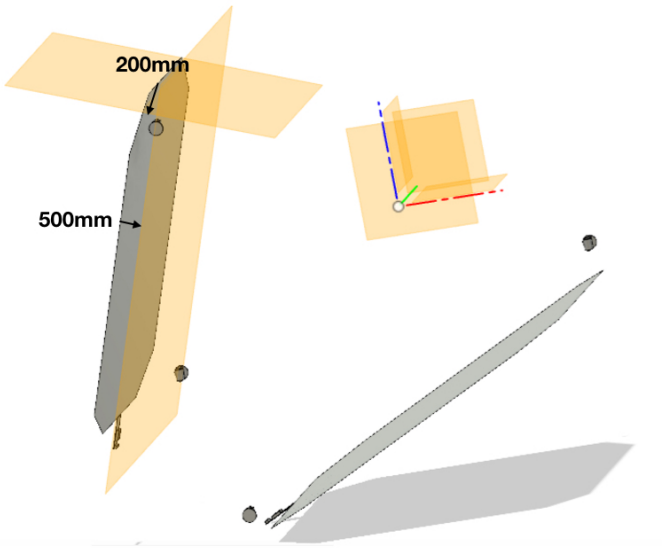

Figure 2.11: *Side view of the tether placement*

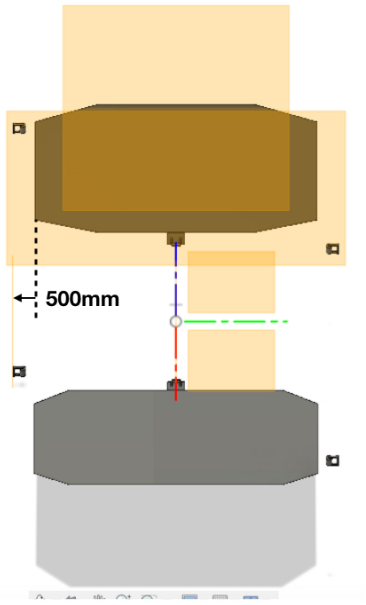

Figure 2.12: *Front view of the tether placement*

When the mirrors are at their normal position, the mounting points has 500mm offset at the normal axis of the mirror surface (pointing outward). Along the mirror surface the mounting locations are 500mm offset outward on the horizontal axis and 200mm offset inward (which means for the upper mounting point will be below the mirrors top edge and the lower one will be above the bottom edge) on the vertical axis. The geometric of the mirror have been simplified into a flat rectangular surface during the design, and the reference points are the corners of the rectangle.

At the robot end, the design needs to assure that the tethers can not interfere with the Puck clearance. The tether connectors should be detachable and ideally the connectors should be able to rotate freely in order to prevent the tethers getting tangled. The mechanical team have found a slip-ring which can not only fulfill the requirements but also allows the power cable to combine with the safety tethers. However the dimensions of the slip-ring is too large to be installed onto the robot, so currently the tethers are connected by a fixed connector.

Safety Reels

2.3.3 Error Budget

The precision requirement on z-axis offset measurement is 1 micrometer and there are multiple sources of uncertainty, including tilting, thermal effects, unfilterable vibrations and the error of the Eddy current sensor itself. The total error will depend on the combination of these factors. In order to transform the precision constraint into the design constraints, the mechanical team (Alex) made this error budget. Several assumptions have been made during the calculations, including: (1) All the uncertainties satisfy the normal distribution (Gaussian distribution); (2) The budget is equally distributed to all factors except sensor error (In future test one may find that one factor has more effect than others and can adjust the quota).

The total budget is 1 micrometers;

1. Eddy current sensor error: From data sheet we know that the resolution is 0.02% of the measured distance, which is 1mm according to the robot design; So the cost due to the sensor error is 0.2 micrometer.

2. Tilting: The other three factors will have equal amount of error budget. From the property of normal distribution we know that:

$$3\sigma_{total} = 0.8\mu m; \sigma_{total} = 0.26667\mu m$$
$$\sigma^2_{total} = 0.07111\mu m^2 = 3\sigma^2_{each}$$
$$\sigma^2_{each} = 0.02370\mu m^2$$

   Using 0.8 micrometer as 3 times the standard deviation, we can assure that the probability for the total error be smaller than 0.8 micron is over 99.7%. According to the geometry of the robot, the relation between the tilt angle and z-axis offset variance is:

$$\frac{s}{L\theta} \approx \frac{L\theta}{L}$$

Therefore

$$\theta^2 \approx \frac{1}{L}s$$

$$\theta^2 \sim N(0, 1.389 \times 10^{-11} rad^4 = N(0, 1.4974 \times 10^{\circ 4})$$

This means during the tilt angle testing, the tilt angle value must lies between [-0.33,0.33] degrees (3 times standard deviation);

3. Thermal effect: The thermal deformation can be considered linear to the temperature change, and use the results from FEA we can find that:

$$s = \frac{1}{10}\Delta T(\mu m)$$

$$T \sim N(0, 2.37^{\circ} C^2)$$

This means the maximum temperature variance allowed during one measuring process is [-4.618,4.618] degrees Celsius;

4. Vibration: The effect on z-axis offset can be considered equal to the amplitude, so the vibration must satisfy that:

$$V \sim N(0, 0.0237 \mu m^2)$$

So the amplitude of the vibrations can not exceed 0.4618 micrometers. However, only the unfilterable vibrations will create uncertainties, and if the frequency of the vibration is 2 times larger than the sampling frequency of the Eddy current sensor it has no effect to our measurement. For the low frequency vibrations we can also filter out their effect in software.

2.3.4 Simulations

FEA for Puck Tower

In order to visualize the effect of thermal-expansion and optimize the design of puck tower, the mechanical team have used ANSYS and Solidworks to do the finite element analysis to the puck tower. The main thermal deformation comes from the temperature difference from the ambient environment. As the ambient temperature heats up or drops down 10 centigrade degrees, the deformation between the center of the puck and the bottom of the probe is required to be less than one micrometers in order to decrease the influence to measurement errors. A finite element analysis including a thermal test and a static test was applied to simulate the deformation for the whole model of puck tower on ANSYS.

- Thermal analysis: Due to the main thermal transfer from the ambient temperature, a convection process was used to determine the temperature changes on the puck tower, and conduction process on puck tower was considered by ANSYS automatically. In fluids, such as air, convection is a much more efficient method of heat transfer than

conduction [2]. Thus, its important to obtain the exact value of convective heat transfer coefficient of air, h, on working space and an approach was used to define h through the Nesselt number Nu which is the ratio between the convective and conductive heat transfer [1]:

$$h_c = \frac{Nu * k}{L}$$

Where k is thermal conductivity and L is the characteristic length of puck tower. The Nusselt number depends on the geometrical shape of the heat sink and on the air flow. For Laminar flow,

$$Nu = 0.59 * Ra^{0.25}$$

Where:

$$Ra = Gr * Pr$$

Is the Rayleigh number defined in terms of Prandtl number (Pr) and Grashof number (Gr). If $Ra < 10^9$ the heat flow is laminar, otherwise if $Ra > 10^9$ the flow is turbulent.

The Grashof (Gr) number is defined as following:

$$Gr = \frac{g * L^3 * \beta * (T_p - T_a)}{\eta^2}$$

And the Prandtl number, Pr, is defined as

$$Pr = \frac{\mu * cp}{k}$$

Where:

- ☐ g = acceleration of gravity = $9.78 m/s^2$ at 5600 meters altitude above sea level.
- ☐ β = air thermal expansion coefficient = $0.00381/K$.
- ☐ Tp = Puck temperature = $-20C$.
- ☐ Ta = Air temperature = $-10C$
- ☐ μ = air dynamic viscosity = $1.6 * 10^{-5} kg/(m * s)$ [3]
- ☐ η = air kinematic viscosity = $2.33 * 10 m^2/s$ [4]
- ☐ cp = air specific heat = $1005 J/(kg * K)$ for dry air
- ☐ k = air thermal conductivity = $0.0224 W/(m * K)$ [4]

Note that all parameters above were determined at altitude of 5600 meters above sea level and ambient temperature of negative 10 centigrade degrees.

Finally, the thermal convective coefficient of air is $2.15 W/(m^2 * K)$. Once obtained the value of the thermal convective coefficient of air and inputted the surrounding temperature as negative 10 degrees and puck initial temperature as negative 20 degrees,

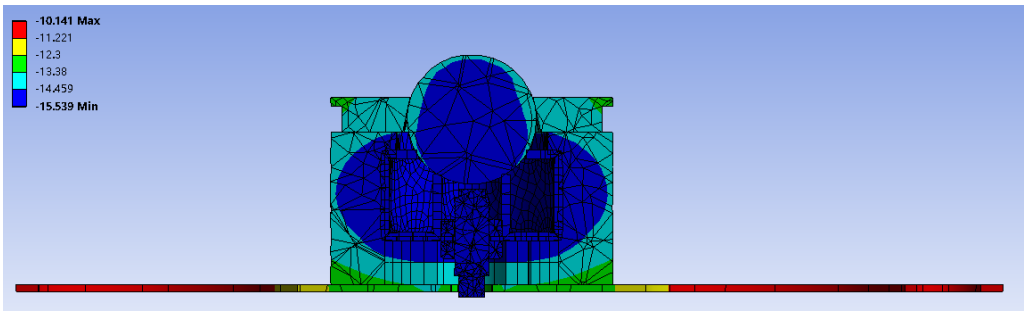

Figure 2.13: *Thermal FEA of puck*

ANSYS could calculate the final temperature of the puck tower assuming that the robot would work at an exposed area in one hour. The result of the FEA is shown in Figure 2.13.

The FEA result above shows the temperature gradient on both puck tower and the base of the robot. Since the base of the robot would also transfer heat to puck tower, its necessary to add it on the whole puck tower model. The base of the robot had the highest final temperature which is close to the ambient temperature because it has the largest area which is exposed to air. The minimum temperature is located at the center of the puck which is remote from the shell of puck tower. The final temperature is not perfectly symmetric because a hole left for cables is inside of puck.

- Statics analysis: Given the inputs of final temperature to statics analysis, ANSYS is able to calculate the deformation by finite element analysis and specific steps are shown below:

  1 : To input the final temperature from the thermal analysis.

  2 : To input all materials and define puck towers parts on ANSYS, the following table shows the corresponding properties to every material.

  3 : To set the boundary conditions for puck tower. In the FEA, the basic plane of robot is fixed on both displacement and rotation.

  4 : To build two body coordinates, which can collect the displacement data with respect to the global coordinate, on center of puck and base of probe.

  5 : Solving FEA and collecting results as shown below.

  As the table shown above, the deformation between center of puck and bottom of probe is 0.95 micrometer which is smaller than one.

  Assuming robot works around an exposure area within one hour and faces 10 centigrade degrees difference to the ambient environment, the deformation from the center of the puck to the bottom of the probe lies within the allowed tolerance, one micrometer. Thus, the design of the structure and applied materials are supposed to work well at the altitude of 5600 meters and -10 centigrade degrees environment.

Table 2.2: *Materials properties of puck tower*

Name	Density (kg/m^3)	Coefficient of thermal expansion $(\mu m/(m * K))$	Young's modulus (GPa)	Poisson ratio
Zerodur	2530	-0.1	84.7	0.25
Commom polymer (ABS)	1000	81.0	3	0.3
Peek	1410	14.0	3.8	0.3
Puck	2500	8.4	70	0.3
Steel	7850	12.0	210	0.3

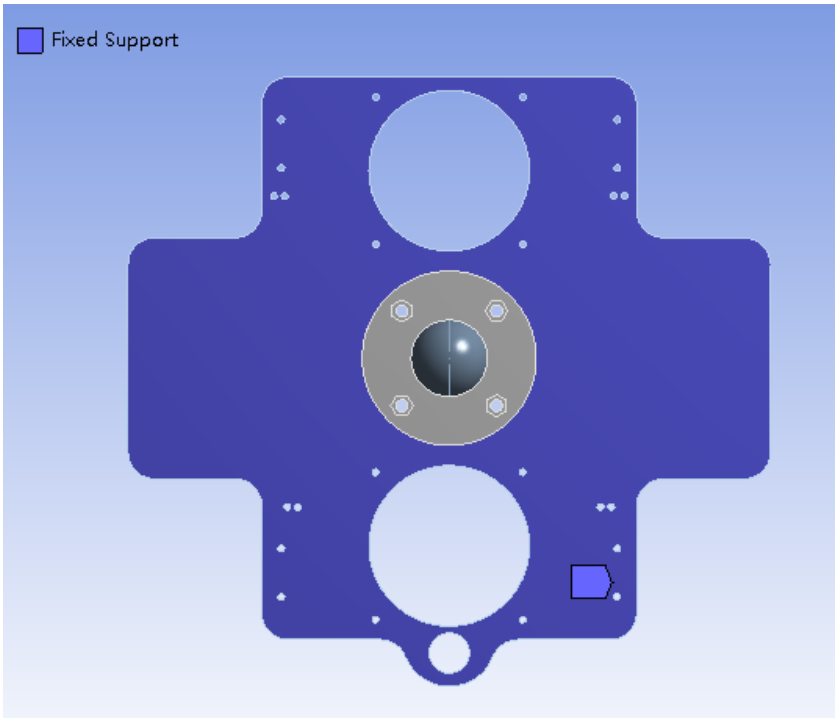

Figure 2.14: *Top view of puck tower model and fixed part shown in blue*

Failure test from tethers pressure

Due to the tensile strength from the tether, its necessary to test the reliability of the puck tower model. Our mechanical team did a failure test on ANSYS forced by tensile stress and thermal stress as well. An approach used is to find the maximum pressure that could be

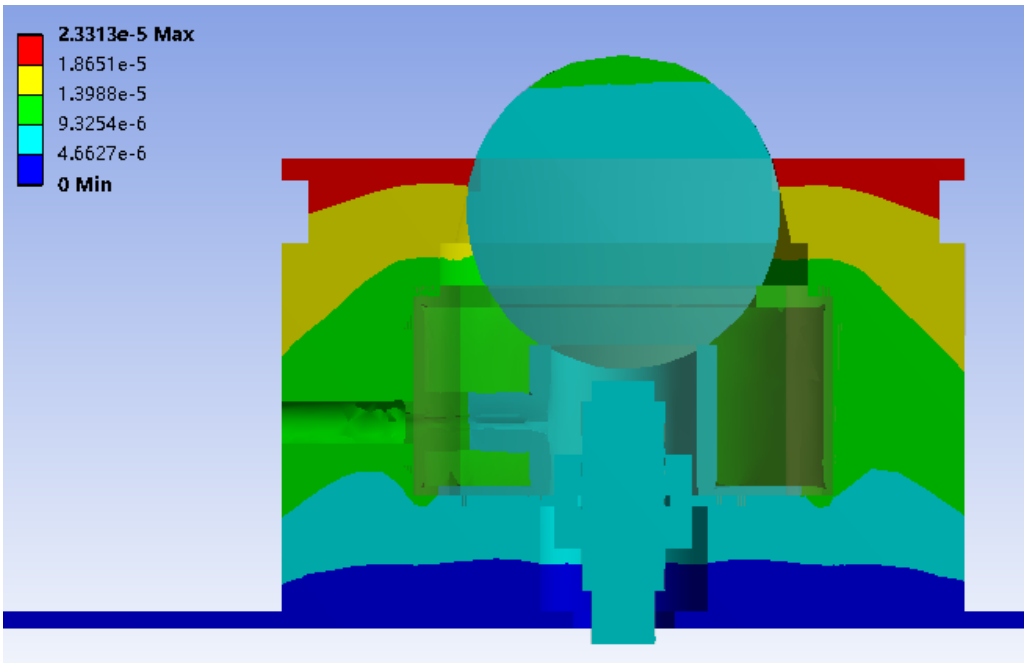

Figure 2.15: *Overall static result on deformation of all parts. The gradient bar is shown on left top corner (units in meter)*

Table 2.3: *The detailed results of deformation between center of puck and bottom of probe*

	Deformation (Z axis) (μm)
Center of the Puck	8.43
Bottom of the probe	7.48
Deformation between center of puck and bottom of probe	0.95

applied on puck tower and to ensure the resulting stress on puck tower would not exceed the yield stress of corresponding materials, ABS. With the same boundary conditions as the thermal analysis, additional pressure was applied on the groove of puck tower, as shown on the figure, and the direction of pressure is shown as the red arrow on the figure 2.16.

Since the yield stress of general ABS has a large range from 13 MPa to 65 MPa, the certain yield stress of puck tower was assumed as 50 MPa. When a 50 MPa tensile pressure is applied on the puck tower, the resulting stress on puck tower is 49 MPa which is less than the yield stress and puck tower is under elastic deformation. Since the tensile stress from the tether, in reality, is much less than 50 MPa, the puck tower is safe to connect by tethers.

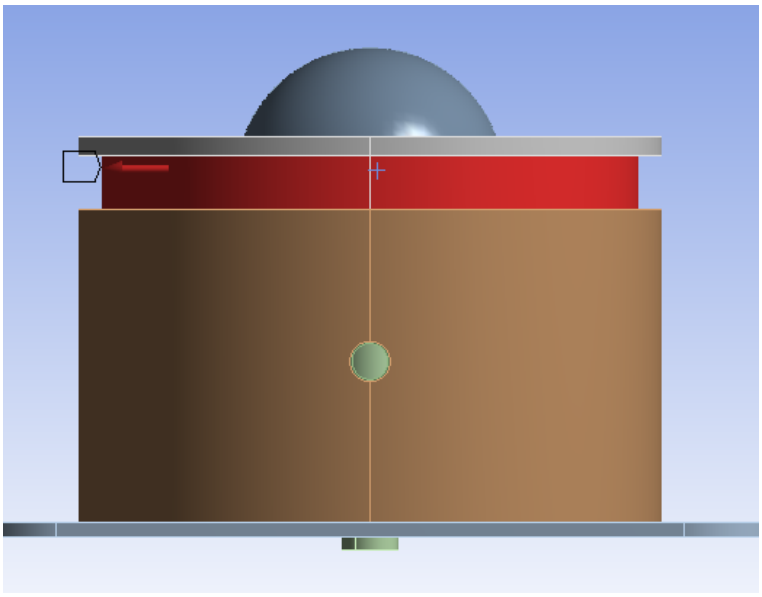

Figure 2.16: *Force condition: tensile pressure applied on the red area of puck tower*

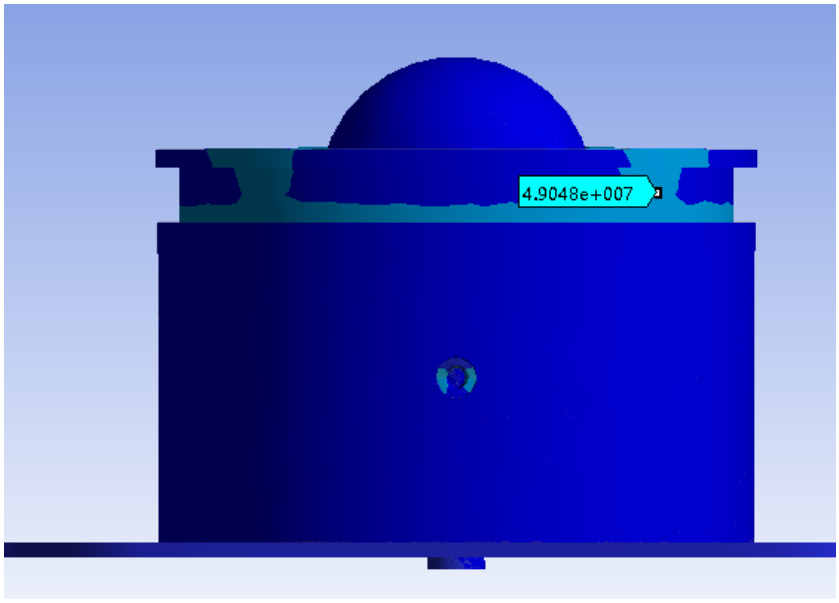

Figure 2.17: *Failure test result: the maximum stress on puck tower (units in Pa)*

Dynamic simulations for tether system

To prevent that the tethered robot swinging back and hitting the mirror, a dynamic simulation have been done to determine the minimum retraction time of the tethers. The minimum retraction time is defined as the time interval between the detachment time and the first time collision occurs (if any). The simulation was done in Matlab, using ODE45 to numerically solve for the motion.

The simulation uses a simplified model of the mirrors, which were modeled as flat rectangular surface with 9 panels on each side (81 panels in each mirror). The secondary mirror is 20 degrees overhung. The robot was modeled as a 1 kg point mass and it is connected to two tether mounting points (their locations are explained above). The tethers are modeled as springs with 100N/m elastic coefficient, the rest length of the tether springs are always equal to its length when the robot is released (which means there are no tensions in the tethers at the time the robot starts to fall). The simulation function will provide an animate of the robot motion and when simulation is done, it will plot the 3D trajectory and tension as a function of time.

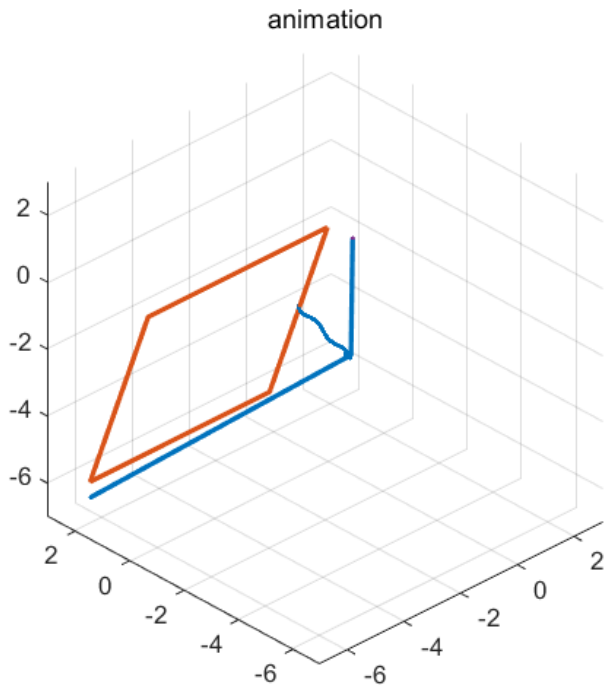

Figure 2.18: *Simulator result for tether system*

According to the simulation result, in any conditions the first collision will not occur in 1.8 seconds, so as long as the tether retraction time is smaller than 1.8 seconds we can assure that the robot will not contact the mirror.

Chapter 3

Results

3.1 Conclusion

3.1.1 Robot construction

In conclusion, the second prototype structural design of the robot was finished during this semester. The CAD model of all parts have been saved in SolidWorks' format and uploaded to the team's Google drive and an exploded view of the most up-to-date robot is shown in Figure 3.1.

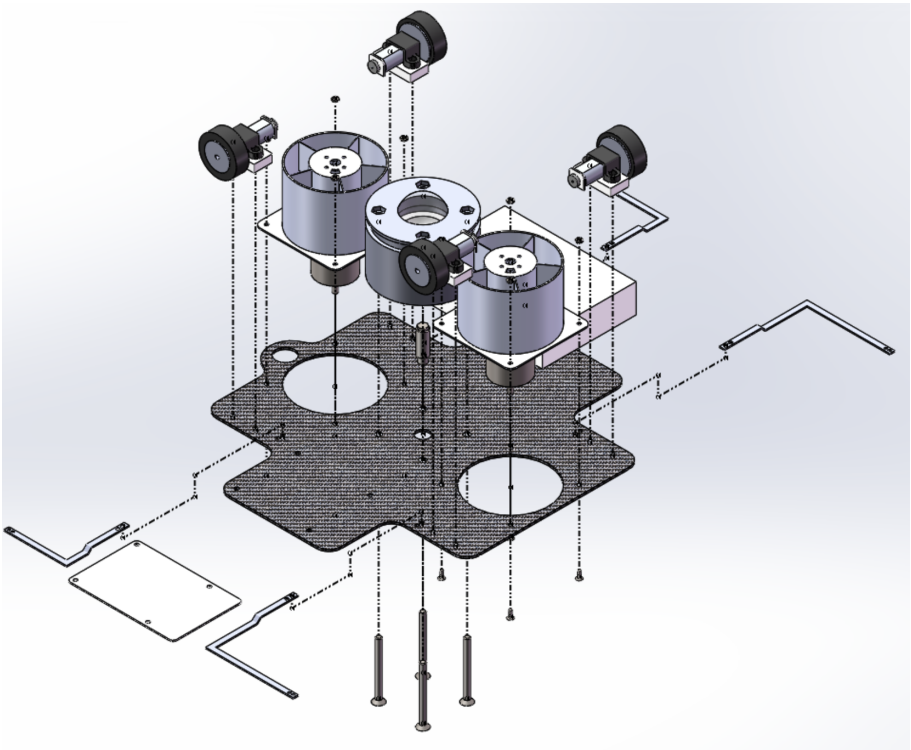

Figure 3.1: *Exploded view of the robot*

A spreadsheet have been made to help keep tracking the status of robot construction.

The first sheet list the on-shelf parts and the second sheet list the parts which need to be manufactured. The details include their names, websites, numbers, materials, weights, unit prizes and current statuses. The spreadsheet is also in the Google drive and it needs timely update to help other team members better understand what is happening.

3.1.2 Simulation test

All simulation testing results including thermal analysis, failure test on puck tower as well as the Dynamic simulations for tether system satisfy the requirements. Thermal analysis and failure test on puck tower are simulated on ANSYS, and tether system simulations are done in Matlab. Working at a 10 centigrade degrees warmer environment, puck tower deforms within an allowed tolerance and the deformation between the center of the puck and the bottom of the probe is only 0.95 micrometer. Made by certain plastic, the puck tower is able to support 50 MPa pressure from tethers. The dynamic simulation in Matlab shows that the robot will not contact the mirror because in any conditions the first collision will not occur in1.8 seconds, so as long as the tether retraction time is smaller than 1.8 seconds.

3.1.3 Future Plan

There are few remaining tasks to be solved in this project. The most important and urgent one is that the fan thrust test have not yielded a successful result yet. Due to the design of the fans and the power of the fan motor, the force output from the current fans do not meet the thrust requirement of the robot. This should be considered as a priority for future work since a system-wide testing is planed at the end of summer 2019. Another important task remaining is the design, manufacturing, and implementation of the tether system. Although the tether simulation proves the dynamics of the tether system, the detailed design and testing of the tethers is yet to be completed. As the safety requirements of this project is an essential part, it is important that the tether and reel systems are tested. Other experiments are also needed in the near future, such as tether connection test, environmental test under low temperature and low atmospheric pressure, and measurement precision test.

Bibliography

[1] D.Roncati. Iterative calculation of the heat transfer coefficient.

[2] D. Durran and Y. Beres. Comparing heat transfer by convection and conduction.

[3] T. engineering toolbox. Properties of us standard atmosphere ranging -5000 to 250000 ft altitude, . URL `https://www.engineeringtoolbox.com/standard-atmosphere-d`$_6$04.*html*.

[4] T. engineering toolbox. International standard atmosphere in elevation -2000 to 30000 metre - pressure, temperature, density, viscosity, thermal conductivity and velocity of sound, . URL `https://www.engineeringtoolbox.com/international-standard-atmosphere-d`$_9$85.*html*.